

~~CONFIDENTIAL~~

UNCLASSIFIED

Copy 6  
RM L50H30a

OCT 18 1950

~~765~~  
218

# RESEARCH MEMORANDUM

DAMPING IN YAW AND STATIC DIRECTIONAL STABILITY OF A  
CANARD AIRPLANE MODEL AND OF SEVERAL MODELS HAVING  
FUSELAGES OF RELATIVELY FLAT CROSS SECTION

By Joseph L. Johnson

Langley Aeronautical Laboratory  
Langley Air Force Base, Va.

CLASSIFICATION CANCELLED

Authority *NACA R7 2565 Date 8/23/54*

By *MDA 9/20/54*

CLASSIFIED DOCUMENT

This document contains classified information affecting the National Defense of the United States within the meaning of the Espionage Act, USC 50-31 and 32. Its transmission or the revelation of its contents in any manner to an unauthorized person is prohibited by law.

Information so classified may be imparted only to persons in the military and naval services of the United States, appropriate civilian officers and employees of the Federal Government who have a legitimate interest therein, and to United States citizens of known loyalty and discretion who of necessity must be informed thereof.

## NATIONAL ADVISORY COMMITTEE FOR AERONAUTICS

WASHINGTON

October 16, 1950

NACA LIBRARY

LANGLEY AIR FORCE BASE  
LANGLEY, VIRGINIA

~~CONFIDENTIAL~~

UNCLASSIFIED



UNCLASSIFIED

NACA RM L50H30a

3 1176 01436 8196

## NATIONAL ADVISORY COMMITTEE FOR AERONAUTICS

## RESEARCH MEMORANDUM

DAMPING IN YAW AND STATIC DIRECTIONAL STABILITY OF A  
CANARD AIRPLANE MODEL AND OF SEVERAL MODELS HAVING  
FUSELAGES OF RELATIVELY FLAT CROSS SECTION

By Joseph L. Johnson

## SUMMARY

An investigation has been made to determine the damping in yaw and static directional stability characteristics for a flat-fuselage model having its major cross-sectional axis either horizontal or vertical, for a flat-fuselage model having its major axis horizontal in combination with a  $45^\circ$  sweptback wing, and for a canard model having a triangular horizontal control surface and a  $45^\circ$  sweptback wing.

The results of the investigation showed that, at high angles of attack, the canard model and the flat-fuselage models with major axis horizontal had negative damping in yaw and positive static directional stability with tails off because of a sidewash which effectively reversed the angle of sideslip over the fuselage. This sidewash caused the directional stability contributed by a vertical tail on the fuselage to be reduced, but it reinforced the yawing flow at the rear of the fuselage so that the damping in yaw contributed by this vertical tail was increased. For the flat fuselage with major axis vertical, the damping in yaw was positive and the static directional stability was negative over the angle-of-attack range, and a vertical tail at the rear of this fuselage contributed a stabilizing increment to both the static and damping derivatives. Wing-tip tails located out of the sidewash field generally increased both the damping in yaw and static directional stability.

## INTRODUCTION

Several investigations have recently been made to determine the static stability of canard airplane models and of several models having fuselages of relatively flat cross section (references 1 to 3). These investigations showed that at the higher angles of attack sidewash from the horizontal control surface of the canard models or from the nose of

UNCLASSIFIED

the flat-fuselage models with major axis horizontal caused an effective reversal in the direction of sideslip of the fuselage which resulted in the models having large positive values of directional stability with vertical tail off. A preliminary analysis indicated that the sidewash over the fuselage occurring at high angles of attack would probably also have an effect on the damping in yaw of these models. Free-oscillation tests were therefore made to determine the values of  $C_{nr}$ , the rate of change of yawing-moment coefficient with yawing angular velocity, for a flat-fuselage model with major axis vertical and also with major axis horizontal (identical to models of reference 1), for a flat-fuselage model with major axis horizontal in combination with a  $45^\circ$  sweptback wing, and for a canard model having a triangular horizontal control surface and  $45^\circ$  sweptback wing. The effect of a vertical tail located at the rear of the fuselage was determined for each model investigated. Tests were also made to determine the static directional stability of some of the configurations studied in the damping tests.

#### SYMBOLS AND COEFFICIENTS

All forces and moments are referred to the stability axes originating at the center of gravity of each model. (See figs. 1 and 2.)

S	wing area, square feet
b	wing span, feet
R	Reynolds number
$\rho$	density of air, slugs per cubic foot
$\alpha$	angle of attack of fuselage center line, degrees
V	airspeed, feet per second
$\psi$	angle of yaw, degrees
$\beta$	angle of sideslip, degrees
r	yawing angular velocity, radians per second
$C_L$	lift coefficient $\left( \frac{\text{Lift}}{\frac{1}{2}\rho V^2 S} \right)$
$C_y$	lateral force coefficient $\left( \frac{\text{Lateral force}}{\frac{1}{2}\rho V^2 S} \right)$

$C_n$	yawing-moment coefficient $\left( \frac{\text{Yawing moment}}{\frac{1}{2} \rho V^2 S b} \right)$
$C_{n\beta}$	rate of change of yawing-moment coefficient with angle of sideslip $(\partial C_n / \partial \beta)$
$C_{nr}$	rate of change of yawing-moment coefficient with yawing angular velocity $\left( \partial C_n / \partial \frac{r b}{2V} \right)$

#### APPARATUS AND MODELS

The free-oscillation tests were conducted in the Langley free-flight tunnel on a stand which permitted the model to have freedom in yaw only. A description of the test apparatus is given in reference 4. Force tests to determine the directional stability of the models were made on the six-component balance in the Langley free-flight tunnel. (See reference 5.)

Three-view drawings of the models are presented in figure 2 and a list of the dimensional characteristics of the models is given in table I.

#### TESTS

Free-oscillation tests were made by the method described in reference 4 to determine the values of the damping-in-yaw derivative  $C_{nr}$  over an angle-of-attack range with vertical tails off and on for each model. All the damping tests were run at a dynamic pressure of 1.2 pounds per square foot which corresponds to an airspeed of approximately 31.2 feet per second at standard sea-level conditions and to an effective Reynolds number range of 171,000 to 275,000 based on the mean aerodynamic chords of the models investigated.

Force tests were made to obtain the directional stability characteristics of the same configurations tested by the free-oscillation method. The static-lateral-stability data presented herein were obtained by determining the difference between moments measured at  $5^\circ$  and  $-5^\circ$  yaw over an angle-of-attack range. In order to determine how well these data represented the variation of the directional stability at higher angles of yaw, the lateral derivatives were also determined for a few conditions from tests made over an angle-of-yaw range from  $20^\circ$  to  $-20^\circ$  at constant angle-of-attack settings. All force tests were made within a dynamic-pressure range from 2.0 to 4.1 pounds per square foot which corresponded

to an effective Reynolds number range from 318,500 to 443,000 based on the mean aerodynamic chord of the models investigated.

All models were tested with and without a vertical tail located at the rear of the fuselage. Models 3 and 4 were tested with and without tip tails and model 3 was tested with leading-edge flaps off and on.

Streamers of string were attached to model 2 to determine the direction of the flow around the model at high angles of attack while the model was oscillating in yaw. A study of the flow around this model for a sideslip condition was made in a previous investigation. (See reference 1.)

## RESULTS AND DISCUSSION

The results of the investigation are presented in terms of the directional-stability parameter  $C_{n\beta}$  and the damping-in-yaw parameter  $-C_{n_r}$ . Since  $C_{n\beta}$  indicates positive directional stability and  $-C_{n_r}$  indicates positive damping, all the results appearing above the origins in the figures represent either positive static stability or positive damping in yaw. The data for the flat-fuselage models (models 1 and 2) are based on an arbitrarily chosen wing having a span of 3.5 feet and an area of 2.98 square feet (fig. 1(a)).

The values of  $C_{n\beta}$  presented in the report were, in most cases, determined from test data obtained at  $5^\circ$  and  $-5^\circ$  yaw. The values of  $C_{n_r}$  were determined from yawing oscillations whose amplitudes ranged from  $20^\circ$  to  $0^\circ$ . The results of some static tests over the yaw range on these models (data not presented), together with the results of references 1 to 3, indicate that the results obtained at  $5^\circ$  and  $-5^\circ$  yaw apply up to yaw angles as high as  $20^\circ$  except in the case in which a vertical tail is located on the fuselage. For this case of the vertical tail on the fuselage the data presented herein were obtained from tests made over the yaw range, and values of  $C_{n\beta}$  and  $C_{n_r}$  are presented for both the low and high angles-of-yaw ranges. The results designated "low  $\psi$ 's" in the figures apply to angles of yaw or amplitudes of the oscillation up to approximately  $15^\circ$  and the results designated "high  $\psi$ 's" apply to angles of yaw or amplitudes of the oscillation between approximately  $10^\circ$  and  $20^\circ$ .

The data of the present investigation as well as those of references 1 to 3, were obtained at low scale ( $R = 171,000$  to  $483,000$ ), but a comparison of these data with the higher scale data obtained at the Ames Aeronautical Laboratory (not generally available) ( $R = 3,700,000$ ,  $M = 1.4$ )

indicate that the results of these low-scale investigations are similar to results obtained at higher Reynolds numbers and Mach numbers.

### Flat-Fuselage Models

(Models 1 and 2)

Results of  $C_{n\beta}$  and  $C_{n_r}$  tests.- The results of tests of the flat-fuselage models with major axis vertical and major axis horizontal are presented in figure 3. The static-directional-stability data for these models were obtained from reference 1. For convenience in presentation, models 1 and 2 of this report have been given opposite designations from those of reference 1.

The model with major axis vertical (model 1) was directionally unstable at low angles of attack and became increasingly unstable as the angle of attack increased. The damping in yaw for this particular model was positive ( $-C_{n_r}$ ) over the angle-of-attack range and increased with increasing angle of attack. With the major axis horizontal (model 2), the model was slightly directionally unstable at low angles of attack but became directionally stable as the angle of attack was increased. The damping in yaw for this configuration was negative over most of the angle-of-attack range and the model became more unstable with increasing angle of attack.

When a vertical tail was placed at the rear of the fuselage with major axis vertical, the contribution to the static stability and damping in yaw was stabilizing at angles of attack of both  $0^\circ$  and  $32^\circ$ . For the fuselage with the major axis horizontal, the vertical tail gave a stabilizing increment to the static stability at  $0^\circ$  angle of attack. At an angle of attack of  $32^\circ$ , however, the sidewash on the fuselage caused the vertical tail to be statically destabilizing at small angles of yaw. At the higher yaw angles the tail was out of the strongest portion of the sidewash field and therefore acted in a normal manner, that is, to give a stabilizing increment to the directional stability. The tail contribution to the damping in yaw was stabilizing for this model at angles of attack of both  $0^\circ$  and  $32^\circ$ . At  $32^\circ$  angle of attack, however, the sidewash at the tail apparently reinforced the yawing flow so that the damping of the tail was much greater than at  $0^\circ$  angle of attack. At  $32^\circ$  angle of attack, the damping of the tail was slightly greater at low angles of yaw than at the high angles of yaw because the tail was partially out of the sidewash field at the higher yaw angles.

Results of flow survey tests.- The results shown in figure 3 can be explained by the diagrams of figure 4, in which the representative flow and forces acting on these models at an angle of attack of  $32^\circ$  are shown in both the static and dynamic conditions. Consider first the fuselage

with major axis vertical in a positive sideslip (fig. 4(a)). The flow over the body caused a side force to the left and, since the center of gravity was rearward to correspond to a canard or tailless-type airplane, this side force produced a negative yawing moment and a statically unstable condition ( $-C_{n\beta}$ ). The flow over the vertical tail at the rear of this fuselage caused a side force to the left which produced a positive yawing moment about the center of gravity, and therefore a stabilizing increment to the directional stability ( $+C_{n\beta}$ ).

When the fuselage with major axis horizontal was in a positive sideslip (fig. 4(b)), the flat nose caused a reversal in the direction of flow over the complete length of the fuselage. This sidewash produced an effective reversal in sideslip which resulted in a side force to the right, even though the model was in a positive sideslip. This side force gave a positive yawing moment about the center of gravity, and hence positive directional stability ( $+C_{n\beta}$ ). The sidewash acted on the vertical tail to give a side force to the right, which produced a negative increment of directional stability ( $-C_{n\beta}$ ). At the higher angles of yaw, the vertical tail moved partly out of the sidewash field and acted in a more normal manner to give a positive increment of static stability.

Presented in figures 4(c) and 4(d) are diagrams showing the two models in positive yawing flow. For the fuselage with major axis vertical (fig. 4(c)) the positive yawing velocity caused a side force to the left that produced a negative yawing moment about the center of gravity. Since this yawing moment was in a direction to oppose the yawing motion, the model had positive damping ( $-C_{nr}$ ). The flow at the rear of the fuselage acted on the vertical tail to give a side force to the right that produced a negative yawing moment and therefore positive damping.

When the fuselage with major axis horizontal (fig. 4(d)) was in positive yawing flow, there was a reversal in the direction of flow at the nose, similar to that found in the static tests, which caused a side force to the right. This side force produced a positive yawing moment about the center of gravity and therefore negative damping ( $+C_{nr}$ ). At the rear of the fuselage the sidewash reinforced the yawing flow so that the side force to the right produced by the vertical tail was greater than that obtained from the vertical tail on the fuselage with major axis vertical. This greater side force therefore caused the damping in yaw to be greater than that obtained from the vertical tail on the fuselage with major axis vertical.

Flat-Fuselage Model with  $45^\circ$  Sweptback Wing

(Model 3)

Leading-edge flap off.- The results of the tests of the model having a flat fuselage with major axis horizontal and a  $45^\circ$  sweptback wing (model 3) are presented in figure 5. The static directional stability of the model with vertical tails off increased from a small negative value at low angles of attack to fairly high positive values at the higher angles of attack in a manner similar to that for the flat fuselage with major axis horizontal (model 2). When the tip tails were added to model 3, a positive increment of directional stability was obtained over the angle-of-attack range.

The damping in yaw of the model with vertical tails off was slightly positive ( $-C_{nr}$ ) at  $0^\circ$  angle of attack but decreased and became negative with increasing angle of attack up to an angle of attack of  $16^\circ$ . With a further increase in angle of attack the damping increased rapidly and had a large positive value at an angle of attack of  $32^\circ$ . A comparison of these results with those for model 2 (fig. 3) shows the same trend up to an angle of attack of about  $16^\circ$ . The fact that the damping again became positive at higher angles of attack for model 3 was attributed to the high drag at the wing tips caused by wing-tip stall. The data of reference 6 indicate that wing drag may contribute an appreciable increment of yawing moment due to yawing. This drag force apparently produced a damping moment which overcame the negative damping of the fuselage and resulted in large values of  $-C_{nr}$  at the high angles of attack. The addition of the tip tails to the model resulted in positive damping over the angle-of-attack range and a stabilizing increment of damping up to an angle of attack of  $22^\circ$ . Beyond this point the damping of this configuration was less than that for the model with all tails off. The reason for the model having greater damping at the higher angles of attack with tails off than with tails on is probably that the tip tails reduced the wing-tip drag which was causing the high damping with tails off.

Leading-edge flap on.- The addition of a leading-edge flap to the model reduced the directional stability in the higher angle-of-attack range with tip tails either on or off. When the model with leading-edge flap on was tested with a vertical tail on the fuselage (and tip tails off), it was found that the sidewash caused the vertical tail to be directionally destabilizing at an angle of attack of  $32^\circ$  for low angles of yaw. At the higher angles of yaw, however, this tail was partially out of the sidewash field and therefore acted in a more normal manner to give a positive increment of  $C_{np}$ . Similar effects of the sidewash field on the center vertical tail were noted for model 2.



The damping in yaw of the model with leading-edge flap on and tip tails either off or on was greater up to an angle of attack of about  $20^\circ$  than that for the model with leading-edge flap off. At the higher angles of attack, however, the damping was less than that for the model with leading-edge flap off and, as in the flap-off case, the damping was greater with tip tails off than the damping with tip tails on. The reduction in damping at the higher angles of attack was attributed to the effect of the leading-edge flap on the drag characteristics of the wing. Preliminary longitudinal force tests indicated that the addition of the leading-edge flap to the model decreased the drag at the high angles of attack and therefore prevented the very large increase in the damping of the wing. When the flap-on configuration was tested with a center tail alone, a very large stabilizing damping increment was obtained, and this increment was about twice as great at low angles of yaw as at the high angles of yaw. This variation with angle of yaw in the damping produced by the vertical tail is much greater than that obtained for model 2.

#### Canard Model

(Model 4)

The results of tests made to determine the directional stability and damping in yaw of the canard configuration having a triangular horizontal control surface and a  $45^\circ$  sweptback wing (model 4) are presented in figure 6. The results show that, for the model with all vertical tails off, the directional stability increased from a negative value at low angles of attack to a fairly high positive value at moderate angles of attack and then decreased slightly with a further increase in angle of attack. The configuration with tip tails on gave positive static stability at low angles of attack, and the tip tails contributed an approximately constant stabilizing increment to the directional stability over the angle-of-attack range. These results indicated that the vertical tails were out of the strongest portion of the sidewash field as in the case of model 3. Results of tests made at low angles of yaw with the center and tip tails (represented by symbol in fig. 6) show less directional stability than with tip tails alone, indicating that the center tail was in the sidewash field and that it contributed a negative increment to the directional stability as in the case of models 2 and 3. No tests were made at the higher angles of yaw for this model in the three tail configurations but, on the basis of results of models 2 and 3, the center tail would be expected to contribute a stabilizing increment in the higher yaw range.

The damping-in-yaw data of figure 6 show a decrease in damping as the angle of attack increased for both the tip-tails-off and tip-tails-on configurations. These results are similar to the results for model 3

over the angle-of-attack range covered by model 4. Since model 4 stalled at a much lower angle of attack than model 3, the tests were made for a lower angle-of-attack range ( $0^\circ$  to  $20^\circ$ ) than that covered with model 3 ( $0^\circ$  to  $32^\circ$ ). At angles of attack above  $20^\circ$  the damping for model 4 should be expected to be similar to that for model 3 because the wings of the two models are identical and because it has been shown that wing-tip drag is an important contributing factor to damping in yaw at high angles of attack (reference 6). As in the case of model 3, the addition of a tail on the fuselage of model 4 increased the damping. There was little difference between the damping at high and at low angles of yaw for the model in the three-tail configuration.

#### CONCLUDING REMARKS

The following conclusions were drawn from the results of the investigation to determine the damping in yaw and static directional stability of a fuselage model having its major axis either horizontal or vertical, a flat-fuselage model in combination with a  $45^\circ$  sweptback wing, and a canard model having a triangular horizontal control surface and  $45^\circ$  sweptback wing:

1. At high angles of attack the flat-fuselage models with major axis horizontal and the canard model had negative damping and positive directional stability with tails off because of a sidewash over the fuselage which effectively reversed the angle of sideslip. This sidewash caused the directional stability contributed by a vertical tail on the fuselage to be reduced, but it reinforced the yawing flow at the rear of the fuselage so that the damping in yaw contributed by this vertical tail was increased.

2. The directional stability of the flat fuselage with major axis vertical was negative and the damping in yaw was positive over the angle-of-attack range. A vertical tail at the rear of this fuselage contributed a stabilizing increment to both the static stability and damping derivatives.

3. Wing-tip tails located out of the sidewash field generally increased both the damping in yaw and the static directional stability.

Langley Aeronautical Laboratory  
National Advisory Committee for Aeronautics  
Langley Air Force Base, Va.

## REFERENCES

1. Bates, William R.: Static Stability of Fuselages Having a Relatively Flat Cross Section. NACA RM L9I06a, 1949.
2. Bates, William R.: Low-Speed Static Lateral Stability Characteristics of a Canard Model Having a  $60^\circ$  Triangular Wing and Horizontal Tail. NACA RM L9J12, 1949.
3. Draper, John W.: Low-Speed Static Stability Characteristics of a Canard Model with a  $45^\circ$  Sweptback Wing and a  $60^\circ$  Triangular Horizontal Control Surface. NACA RM L50G11, 1950.
4. Campbell, John P., and Mathews, Ward O.: Experimental Determination of the Yawing Moment Due to Yawing Contributed by the Wing, Fuselage, and Vertical Tail of a Midwing Airplane Model. NACA ARR 3F28, 1943.
5. Shortal, Joseph A., and Draper, John W.: Free-Flight-Tunnel Investigation of the Effect of the Fuselage Length and the Aspect Ratio and Size of the Vertical Tail on Lateral Stability and Control. NACA ARR 3D17, 1943.
6. Toll, Thomas A., and Queijo, M. J.: Approximate Relations and Charts for Low-Speed Stability Derivatives of Swept Wings. NACA TN 1581, 1948.

TABLE I

## DIMENSIONAL CHARACTERISTICS OF MODELS USED IN LANGLEY

## FREE-FLIGHT-TUNNEL INVESTIGATION

## Fuselage Model with Major Cross-Sectional

## Axis Vertical or Horizontal

(Models 1 and 2)

## Fuselage:

Over-all length, ft	4.00
Cross section	Elliptical
Plan form { Model 1	NACA 0007
Model 2	NACA 0014
Side elevation { Model 1	NACA 0014
Model 2	NACA 0007
Volume, cubic ft	0.271

## Vertical tail:

Area, sq ft	0.272
Span, ft	0.73
Root chord, ft	0.495
Taper ratio	0.505
Aspect ratio	1.96

Canard and Flat-Fuselage Models Having a  $45^\circ$  Sweptback Wing

(Models 3 and 4)

## Wing:

Airfoil section	NACA 0012
Area, sq ft	5.33
Span, ft	4.0
Aspect ratio	3.00
Incidence, deg	0
Dihedral, deg	0
Taper ratio	0.5
M.A.C., ft	1.383
Root chord, ft	1.77

## Tip tails:

Area, sq ft (2 tails)	0.533
Span, ft	0.63
Root chord, ft	0.562
Taper ratio	0.50
Aspect ratio	1.49

TABLE I

## DIMENSIONAL CHARACTERISTICS OF MODELS USED IN LANGLEY

## FREE-FLIGHT-TUNNEL INVESTIGATION - Concluded

## Center tail:

Area, sq ft	0.272
Span, ft	0.73
Root chord, ft	0.495
Taper ratio	0.505
Aspect ratio	1.96

## Horizontal control surface (canard model (model 4) only):

Airfoil section	Flat plate
Area, sq ft	0.800
Span, ft	1.36
Sweepback, L.E.	60°
Aspect ratio	2.31



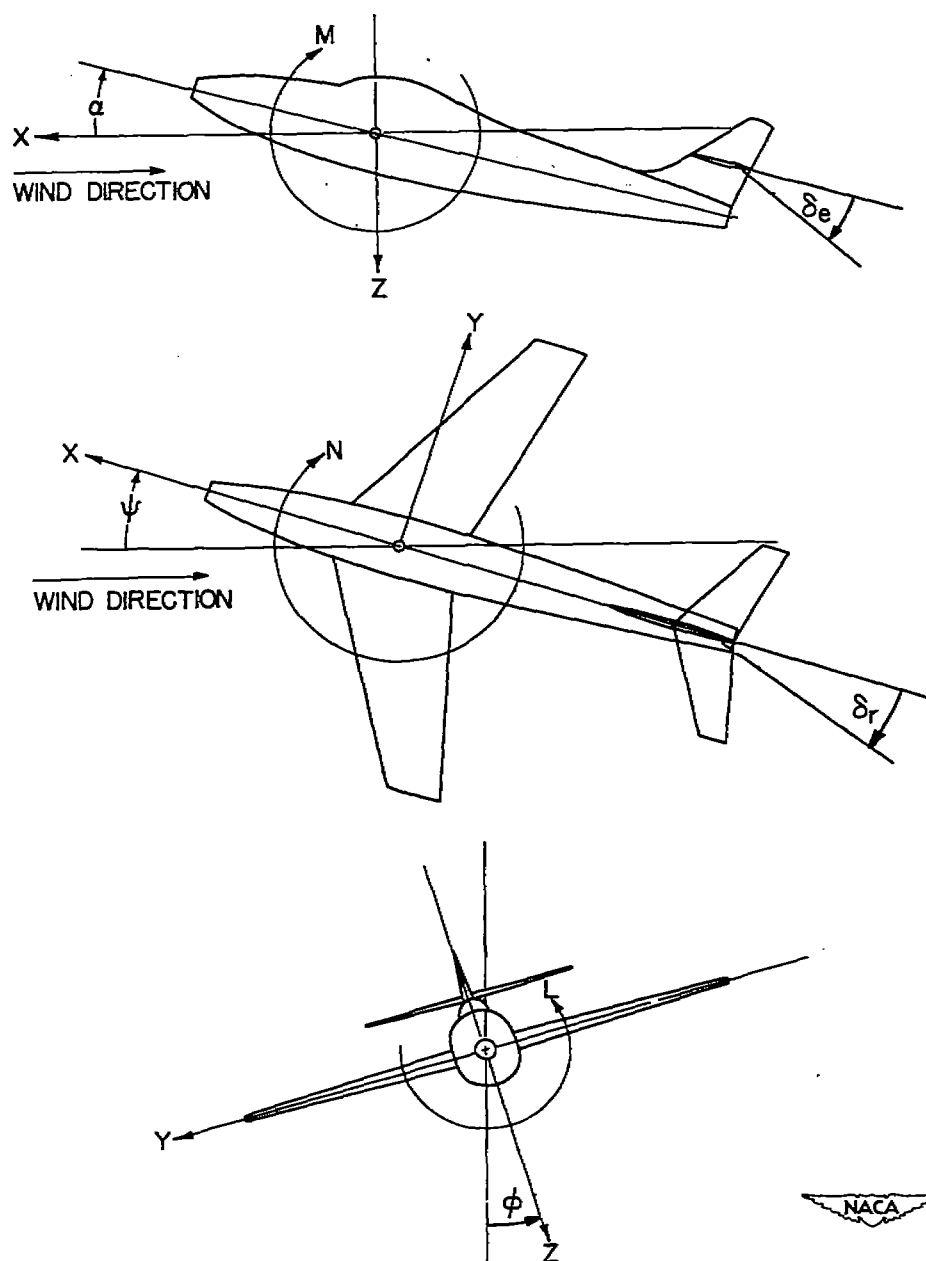


Figure 1.- The stability system of axes. Arrows indicate positive directions of moments, forces, and control-surface deflections. This system of axes is defined as an orthogonal system having the origin at the center of gravity and in which the Z-axis is in the plane of symmetry and perpendicular to the relative wind; the X-axis is in the plane of symmetry and perpendicular to the Z-axis, and the Y-axis is perpendicular to the plane of symmetry.

*Note: Fuselage data  
based on wing  
shown in dotted  
outline.*

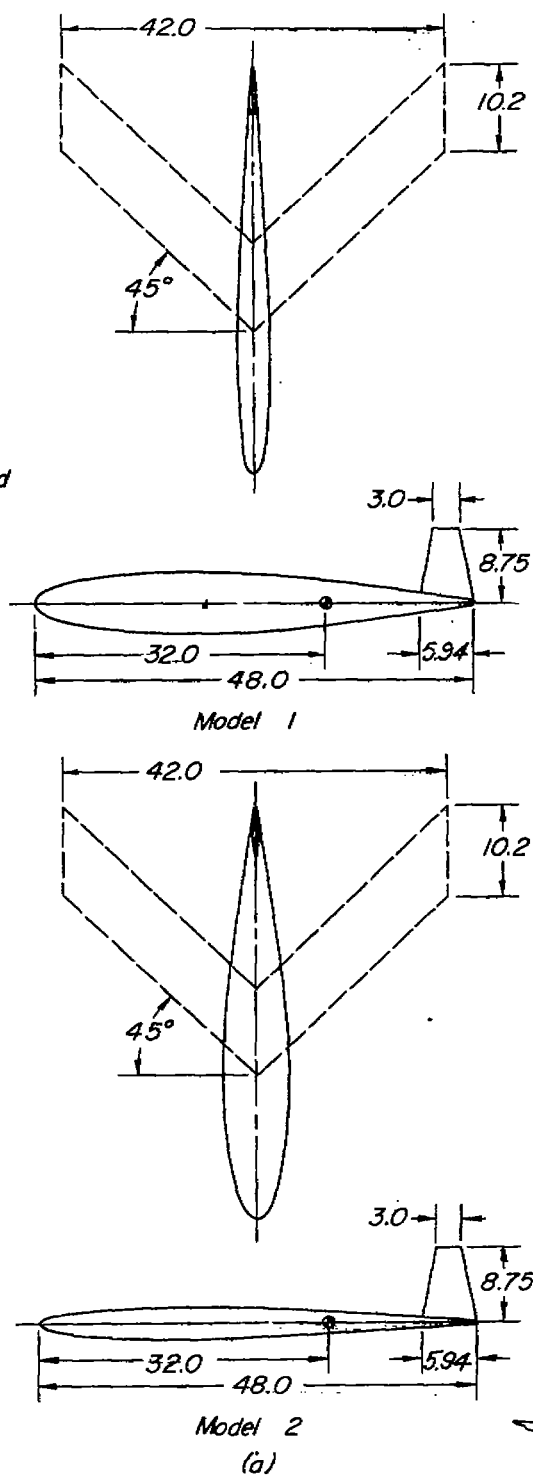
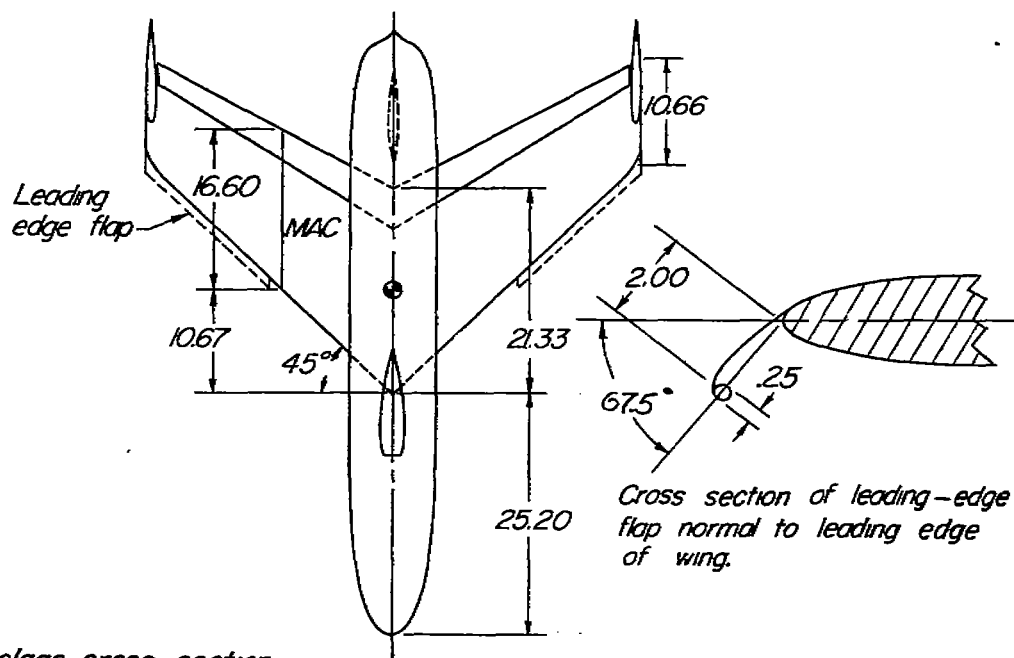
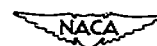
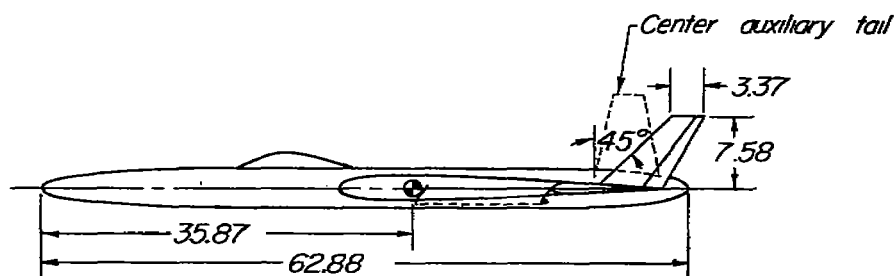
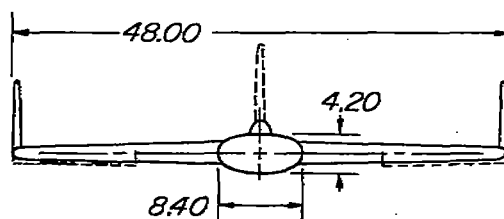


Figure 2.- Models used in the investigation. (All dimensions in inches.)



Note: Fuselage cross-section elliptical



(b) Model 3

Figure 2.- Continued.



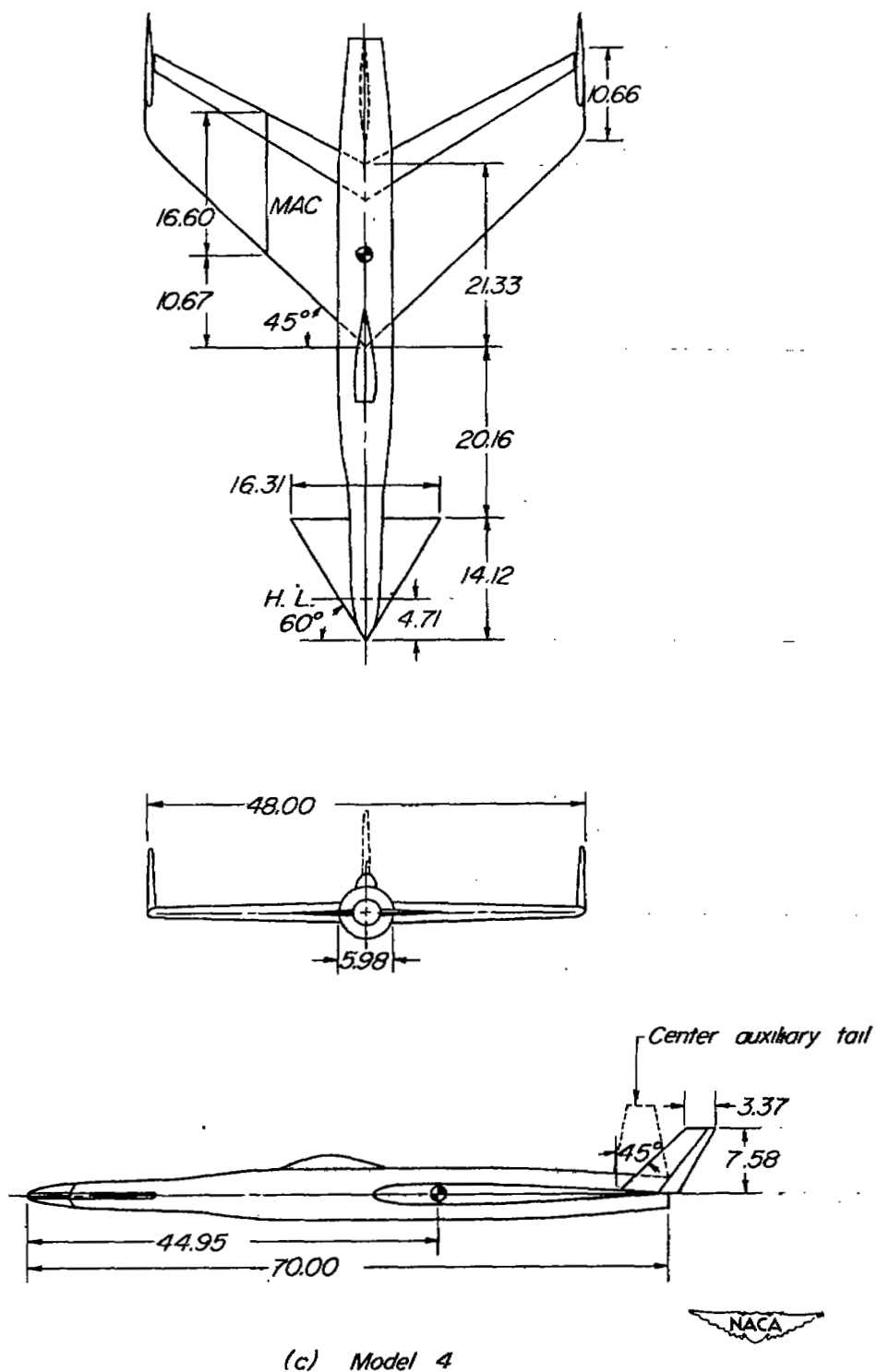


Figure 2.- Concluded.

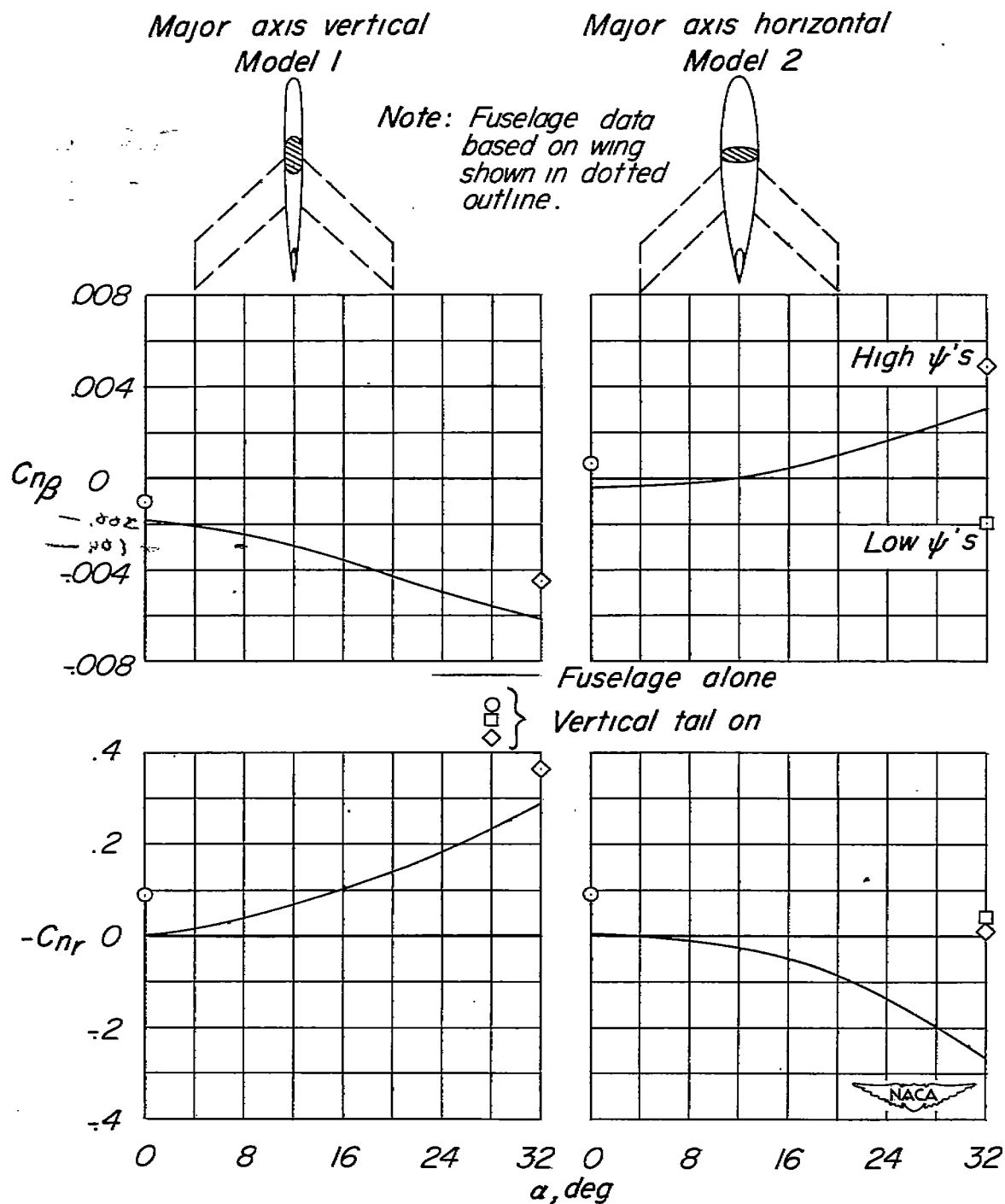


Figure 3.- Static directional stability and damping in yaw of models 1 and 2.

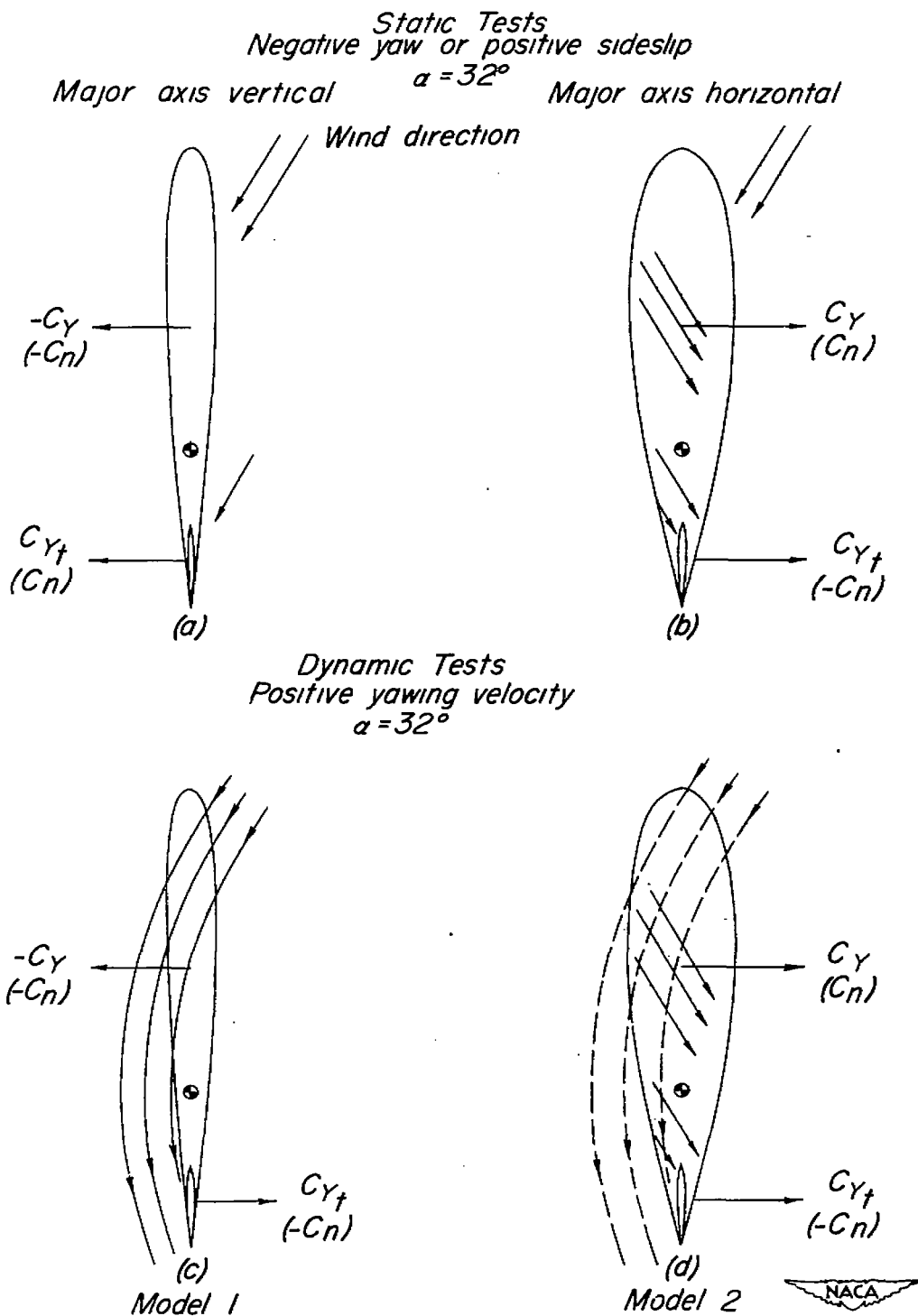
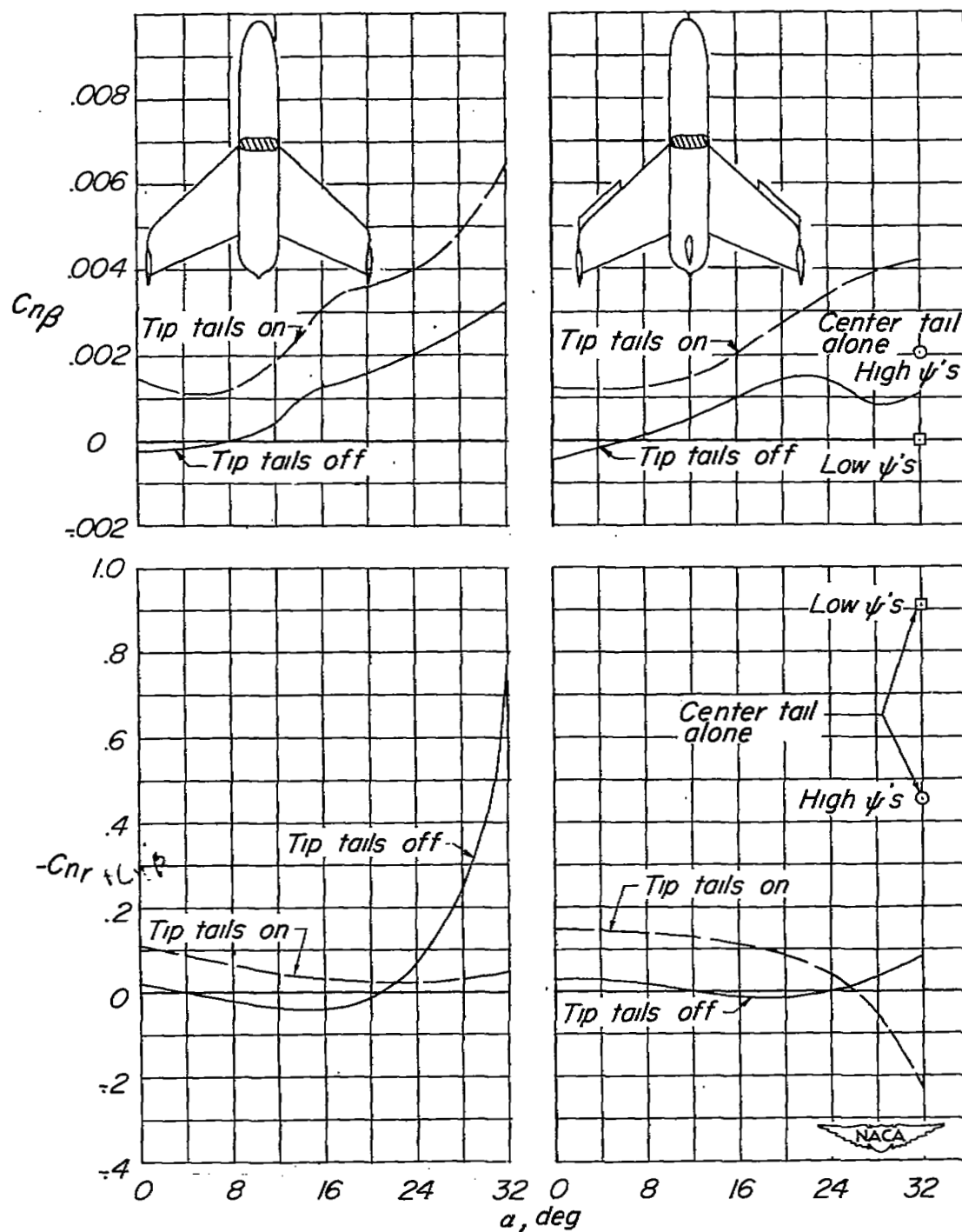


Figure 4.- Representative flow and forces acting on models 1 and 2 in static and dynamic condition.



(a) Leading-edge flap off.

(b) Leading-edge flap on.

Figure 5.- Static directional stability and damping in yaw of model 3.

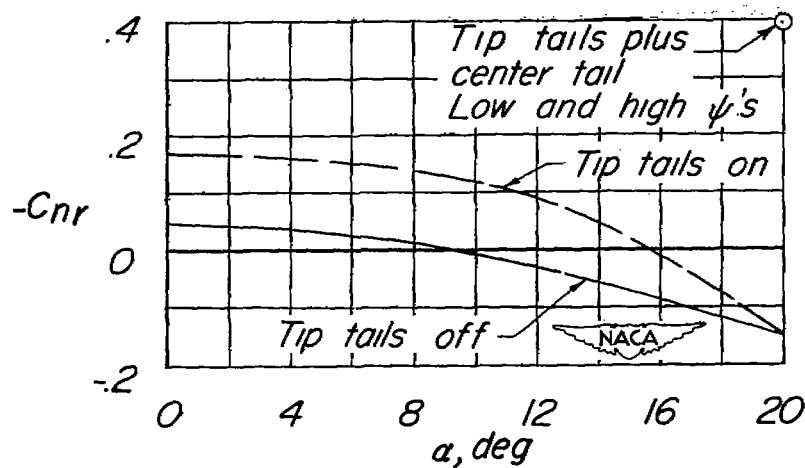
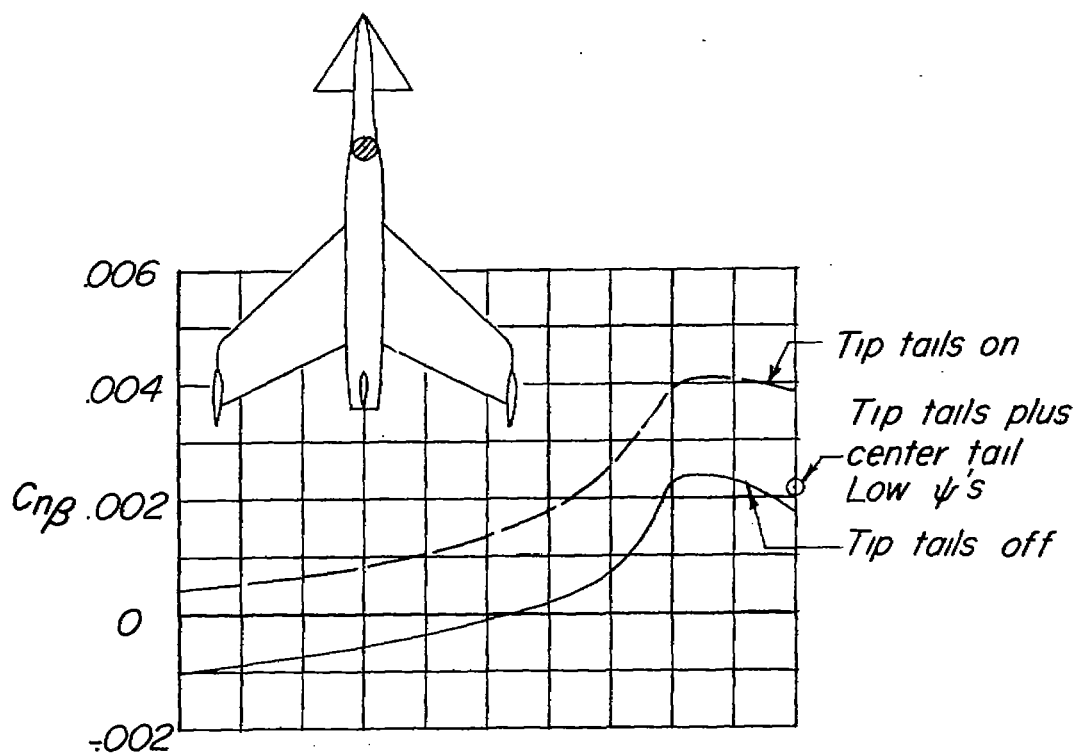


Figure 6.- Static directional stability and damping in yaw of model 4.

NASA Technical Library



3 1176 01436 8196